Vol 11 No 3, March 2002
1009-1963/2002/11(03)/0277-05
Chinese Physics
© 2002 Chin. Phys. Soc.
and IOP Publishing Ltd

Dielectric effect on the rf characteristics of a helical groove travelling wave tube*

Wei Yan-Yu(魏彦玉)[a)†], Wang Wen-Xiang(王文祥)[a)], Sun Jia-Hong(孙嘉鸿)[a)], Liu Sheng-Gang(刘盛纲)[a)], Baofu Jia[a)b)], and Gun-Sik Park[b)]

[a)] *National Key Laboratory of High Power Vacuum Electronics, University of Electronic Science and Technology of China, Chengdu 610054, China*

[b)] *Vacuum Electrophysical National Laboratory, Department of Physics, Seoul National University, Korea*

(Received 14 February 2001; revised manuscript received 2 November 2001)

A new type of partial-dielectric-loaded helical groove slow-wave structure (SWS) for millimetre wave travelling wave tube (TWT) is presented in this paper. The radio-frequency characteristics including the dispersion properties, the longitudinal electric field distribution and the beam-wave coupling impedance of this structure are analysed. The results show that the dispersion of the helical groove circuit is weakened, the phase velocity is reduced and the position of the maximum E_z is moved from the mouth to the inside of the groove after partially filling the dielectric materials in the helical groove SWS. Therefore, the dielectric-loaded helical groove SWS is suitable for a multi-beam TWT with broad band and high gain.

Keywords: dielectric-loading, helical groove waveguide, slow wave structure, travelling wave tube
PACC: 7170G, 7145L, 7110

1. Introduction

During the development of a high-power broad band travelling wave tube (TWT), attention has been newly focused on the whole-metal slow-wave structures (SWS),[1] such as the helical groove waveguide,[2] coaxial radial line, serpentine waveguide and π-type line, etc, due to their super power capability and potential broad bandwidth characteristics. The helical groove waveguide is one of the most important whole-metal SWS for millimetre wave TWT. There are several peculiar characteristics, such as the large transverse size, the high precision of manufacturing and assembly, the perfect wholeness and stability in the structure. The helical groove waveguide was first investigated as a SWS in 1957 by Waldron.[3] Later, Nwachuku[4] and Foulds and Mansell[5] delivered contributions to the circuit. In 1988, the first experimental ridge-loaded helical groove millimetre wave TWT was carried out at the Raytheon Company,[6] and the theoretical study was presented by the authors in 1997.[2] Previous works[2−7] have shown that the bandwidth of the helical groove waveguide is narrow. The instantaneous bandwidth of Raytheon's tube is only 1.3%.[6] Therefore, it is necessary to broaden the band of this structure. Although much work has been done on the different types of helical groove waveguide,[8,9] an investigation of the dielectric-loaded helical groove waveguide, as far as we know, has not appeared in the literature. Recently, the problems associated with dielectric-loaded TWT for the advanced accelerator have become more attractive.[10,11] In this paper, we study the partial-dielectric-loaded helical groove waveguide as a slow-wave circuit for TWT. By partially filling the groove with dielectric materials, the dispersion of the SWS becomes weak, i.e. there is a small phase velocity change of the electromagnetic wave in the partial-dielectric-loaded helical groove waveguide within a broad frequency region. This leads to an effective interaction between the beam and slow waves in the circuit with a relatively wider band. After partially filling the helical groove SWS with dielectric materials, the position of the maximum E_z is changed from the mouth to the inside of the groove. To increase the interaction impedance, several holes are drilled on the inside wall of the groove and the beam is put through the holes. Therefore, the partially-dielectric-loaded helical groove SWS is suitable for multi-beam TWT.

*Project supported by the Fund of the Institute of Electronics Science of the Ministry of Electron Industry (Grant No DJ3.1.1.2).
†E-mail: yywei@uestc.edu.cn; Phone: 028-3201064; Fax: 028-3201709.

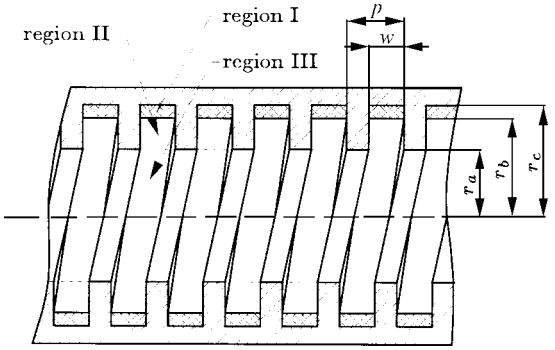


Fig.1. The longitudinal cross section of the partially-dielectric-loaded helical groove waveguide.

2.Dispersion and impedance

2.1. Field components

Figure 1 shows the longitudinal section through the axis of the partially-dielectric-loaded helical groove slow-wave circuit. The groove region is partially filled with lossless dielectric materials from r_b to r_c. The relative permittivity of the material is ε_r. In Fig.1, p and w represent the pitch and groove breadth, respectively, and r_c, r_b and r_a indicate the outer radii of regions I, II and III, respectively. In the following analysis, the pitch is assumed to be sufficiently small compared with the wavelength so that the high-order evanescent modes in the groove regions I and II may be neglected. For the field expressions obtained by employing the approximate helical coordinate system (r, θ, ξ)[5] (one may also use the developed helical coordinate system[12]), the field components of the fundamental TE mode in the helical groove waveguide can be written as follows.

In region I: $(r_b \le r \le r_c)$

$$E_\xi^{\mathrm{I}} = AU(k_1 r)\mathrm{e}^{-\mathrm{j}v\theta}, \tag{1a}$$

$$H_r^{\mathrm{I}} = (v/r\omega\mu_0)AU(k_1 r)\mathrm{e}^{-\mathrm{j}v\theta}, \tag{1b}$$

$$H_\theta^{\mathrm{I}} = -\mathrm{j}(k_1/\omega\mu_0)AU'(k_1 r)\mathrm{e}^{-\mathrm{j}v\theta}, \tag{1c}$$

$$E_r^{\mathrm{I}} = E_\theta^{\mathrm{I}} = H_\xi^{\mathrm{I}} = 0. \tag{1d}$$

In region II: $(r_a \le r \le r_b)$

$$E_\xi^{\mathrm{II}} = BV(kr)\mathrm{e}^{-\mathrm{j}v\theta}, \tag{2a}$$

$$H_r^{\mathrm{II}} = (v/r\omega\mu_0)BV(kr)\mathrm{e}^{-\mathrm{j}v\theta}, \tag{2b}$$

$$H_\theta^{\mathrm{II}} = -\mathrm{j}(k_1/\omega\mu_0)BV'(kr)\mathrm{e}^{-\mathrm{j}v\theta}, \tag{2c}$$

$$E_r^{\mathrm{II}} = E_\theta^{\mathrm{II}} = H_\xi^{\mathrm{II}} = 0. \tag{2d}$$

Here

$$U(k_1 r) = \frac{J_v(k_1 r_c)J_{-v}(k_1 r) - J_{-v}(k_1 r_c)J_v(k_1 r)}{J_v(k_1 r_c)J_{-v}(k_1 r_b) - J_{-v}(k_1 r_c)J_v(k_1 r_b)},$$

$$U'(k_1 r) = \frac{J_v(k_1 r_c)J'_{-v}(k_1 r) - J_{-v}(k_1 r_c)J'_v(k_1 r)}{J_v(k_1 r_c)J_{-v}(k_1 r_b) - J_{-v}(k_1 r_c)J_v(k_1 r_b)},$$

$$V(kr) = \frac{J_{-v}(k_0 r) - G_0 J_v(k_0 r)}{J_{-v}(k_0 r_b) - G_0 J_v(k_0 r_b)},$$

$$V'(kr) = \frac{J'_{-v}(k_0 r) - G_0 J'_v(k_0 r)}{J_{-v}(k_0 r_b) - G_0 J_v(k_0 r_b)},$$

$$k_1 = \omega\sqrt{\varepsilon_r\varepsilon_0\mu_0} = k_0\sqrt{\varepsilon_r}, \quad k_0 = \omega\sqrt{\varepsilon_0\mu_0}.$$

A, B and G_0 are the field amplitude coefficients, $J_{\pm v}(x)$ represents the Bessel function of first kind with order $\pm v$, and $J'_{\pm v}(x)$ represents the first derivative of $J_{\pm v}(x)$ with respect to x. k_0 is the free-space propagation constant, and v is the angular propagation coefficient for waves propagating round the groove. It can be determined by the fact that the phase shift per pitch in the centre region should be equal to the phase change per turn in the groove, i.e. $v = \beta_0 p/2\pi$. Here β_0 is the axial phase propagation constant in the centre region.

The field components in the centre region can be obtained by the Floquet theorem

$$E_z^{\mathrm{III}} = \sum_{m=-\infty}^{\infty} C_m\gamma_m^2 F_m(\gamma_m r)\mathrm{e}^{\mathrm{j}(m\phi-\beta_m z)}, \tag{3a}$$

$$E_r^{\mathrm{III}} = \pm\mathrm{j}\sum_{m=-\infty}^{\infty}[C_m\gamma_m\beta_m F'_m(\gamma_m r) - D_m(m\omega\mu_0/r)F_m(\gamma_m r)]\mathrm{e}^{\mathrm{j}(m\phi-\beta_m z)}, \tag{3b}$$

$$E_\phi^{\mathrm{III}} = \mp\sum_{m=-\infty}^{\infty}[C_m(m\beta_m/r)F_m(\gamma_m r) - D_m\omega\mu_0\gamma_m F'_m(\gamma_m r)]\mathrm{e}^{\mathrm{j}(m\phi-\beta_m z)}, \tag{3c}$$

$$H_z^{\mathrm{III}} = \mathrm{j}\sum_{m=-\infty}^{\infty} D_m\gamma_m^2 F_m(\gamma_m r)\mathrm{e}^{\mathrm{j}(m\phi-\beta_m z)}, \tag{3d}$$

$$H_r^{\mathrm{III}} = \pm\sum_{m=-\infty}^{\infty}[C_m(mk^2/r\omega\mu_0)F_m(\gamma_m r) - D_m\gamma_m\beta_m F'_m(\gamma_m r)]\mathrm{e}^{\mathrm{j}(m\phi-\beta_m z)}, \tag{3e}$$

$$H_\phi^{\mathrm{III}} = \pm\mathrm{j}\sum_{m=-\infty}^{\infty}[C_m(k^2\gamma_m/\omega\mu_0)F'_m(\gamma_m r) - D_m(m\beta_m/r)F_m(\gamma_m r)]\mathrm{e}^{\mathrm{j}(m\phi-\beta_m z)}. \tag{3f}$$

Here C_m and D_m are the field amplitude factors of the mth space harmonic. β_m and γ_m are its axial

and radial propagation constants, respectively. They are defined as $\beta_m = \beta_0 + 2m\pi/p$, $\gamma_m^2 = |\beta_m^2 - k^2|$. If $\beta_m^2 - k^2 > 0$, $F_m(\gamma_m r) = I_m(\gamma_n r)$ and the upper sign of "$\pm$" or "$\mp$" is selected; if $k^2 - \beta_m^2 > 0$, $F_m(\gamma_m r) = J_m(\gamma_m r)$ and the lower sign of "$\pm$" or "$\mp$" is chosen. J_m and I_m represent Bessel and modified Bessel functions of order m, respectively.

2.2. Dispersion equation

At $r = r_b$, the tangential E-fields and H-fields are continuous

$$E_\xi^{\mathrm{I}} = E_\xi^{\mathrm{II}}, \tag{4}$$

$$H_\theta^{\mathrm{I}} = H_\theta^{\mathrm{II}}, \tag{5}$$

while at $r = r_a$, the matching conditions of E-fields are

$$E_\xi^{\mathrm{II}} = E_\xi^{\mathrm{III}}, \tag{6}$$

$$E_\theta^{\mathrm{II}} = E_\theta^{\mathrm{III}} = 0. \tag{7}$$

H_θ-fields should be continuous at the boundary across the groove

$$\int_{Np}^{(N+1)p} H_\theta^{\mathrm{II}} \mathrm{d}z = \int_{Np}^{(N+1)p} H_\theta^{\mathrm{III}} \mathrm{d}z. \tag{8}$$

From Eqs.(4)–(8), the following dispersion equation of the partially-dielectric-loaded helical groove SWS can be obtained

$$\begin{aligned}&\frac{kP_v(k_1r_c,k_1r_b)T_v(kr_b,kr_a)+k_1Q_v(k_1r_c,k_1r_b)R_v(kr_a,kr_b)}{kP_v(k_1r_c,k_1r_b)R_v(kr_b,kr_a)+k_1Q_v(k_1r_c,k_1r_b)P_v(kr_a,kr_b)}\\ &\pm\frac{w}{p}\sum_{m=-\infty}^{\infty}\frac{k}{\gamma_m}\left[\frac{F_m'(\gamma_m r_a)}{F_m(\gamma_m r_a)}-\frac{1}{k\gamma_m}\frac{F_m(\gamma_m r_a)}{F_m'(\gamma_m r_a)}\left(\frac{m\beta_m}{r_a}\mp\gamma_m^2\,\mathrm{tg}\,\Psi\right)^2\right]\\ &\times\left(\frac{\sin\beta_m w/2}{\beta_m w/2}\right)^2=0,\end{aligned} \tag{9}$$

where the functions $P_v(x,y)$, $Q_v(x,y)$, $R_v(x,y)$ and $T_v(x,y)$ are defined as follows

$$P_v(x,y) = J_v(x)J_{-v}(y) - J_{-v}(x)J_v(y),$$

$$Q_v(x,y) = J_v(x)J'_{-v}(y) - J_{-v}(x)J'_v(y),$$

$$R_v(x,y) = J'_v(x)J_{-v}(y) - J'_{-v}(x)J_v(y),$$

$$T_v(x,y) = J'_v(x)J'_{-v}(y) - J'_{-v}(x)J'_v(y).$$

$J_{-v}(k_0r)$ should be replaced by $Y_n(k_0r)$ in the above equations when v is an integer n. For the device without dielectric-loading, i.e. ε_r=1, Eq.(9) can be completely identified with the results given by Foulds and Mansell[5].

2.3. Coupling impedance

The coupling impedance is an important parameter that describes how strong the beam–wave interaction is in a TWT. From Pierce's theory,[13] the coupling impedance of the mth space harmonic is defined as

$$K_c(m) = \frac{E_{zm}E_{zm}^*}{2\beta_m^2 P}, \tag{10}$$

where E_{zm} is the longitudinal component of the electric field of the mth space harmonic at the position r_e of the electronic beam, and E_{zm}^* is its conjugate value. According to Eq.(3a) and the relation between C_m and B, we have

$$\begin{aligned}E_{zm}E_{zm}^* =&\left(\frac{w}{p}B\right)^2\left[\frac{J_{-v}(kr_a)-G_0J_v(kr_a)}{J_{-v}(kr_b)-G_0J_v(kr_b)}\right]^2\\ &\times\frac{F_m^2(\gamma_m r_e)}{F_m^2(\gamma_m r_a)}\left[\frac{\sin(\beta_m w/2)}{\beta_m w/2}\right]^2.\end{aligned} \tag{11}$$

In Eq.(10), P is the total power flow through the whole circuit system

$$P = P^{\mathrm{I}} + P^{\mathrm{II}} + \sum_{m=-\infty}^{\infty} P_m^{\mathrm{III}}, \tag{12}$$

where P^{I} and P^{II} are the power flows in regions I and II, respectively. P_m^{III} is the power flow of the mth space harmonic in space III. The expressions of P^{I}, P^{II} and P^{III} are

$$\begin{aligned}P^{\mathrm{I}} =&\frac{1}{2}w\int_{r_b}^{r_c}E_\xi^{\mathrm{I}}H_r^{*\mathrm{I}}\mathrm{d}r\\ =&\frac{1}{2}wA^2\frac{v}{\omega\mu_0}\int_{r_b}^{r_c}\frac{\mathrm{d}r}{r}\\ &\times\left[\frac{J_v(k_1r_c)J_{-v}(kr)-J_{-v}(k_1r_c)J_v(kr)}{J_v(k_1r_c)J_{-v}(kr_b)-J_{-v}(k_1r_c)J_v(kr_b)}\right]^2.\end{aligned}$$

After evaluating this new type of integral, the expres-

sion becomes

$$P^{\mathrm{I}} = \frac{wA^2}{4\omega\mu_0}\frac{1}{[J_v(k_1r_c)J_{-v}(k_1r_b) - J_{-v}(k_1r_c)J_v(k_1r_b)]^2} \times \Bigg\{k_1r_b\Bigg\{[J_v(k_1r_c)J_{-(v+1)}(k_1r_b) + J_{-v}(k_1r_c) \times J_{v+1}(k_1r_b)]\frac{\partial}{\partial v}[J_v(k_1r_c)J_{-v}(k_1r_b) - J_{-v}(k_1r_c)J_v(k_1r_b)] - [J_v(k_1r_c)J_{-v}(k_1r_b) - J_{-v}(k_1r_c)J_v(k_1r_b)]\frac{\partial}{\partial v}[J_v(k_1r_c)J_{-(v+1)}(k_1r_b) + J_{-v}(k_1r_c)J_{v+1}(k_1r_b)]\Bigg\} - [J_v(k_1r_c)J_{-v}(k_1r_b) - J_{-v}(k_1r_c)J_v(k_1r_b)]^2\Bigg\}. \quad (13)$$

Similarly

$$P^{\mathrm{II}} = \frac{1}{2}w\int_{r_a}^{r_b} E_\xi^{\mathrm{II}}H_r^{*\mathrm{II}}\mathrm{d}r = \frac{wB^2}{4\omega\mu_0}\frac{1}{[J_{-v}(kr_b) - G_0J_v(kr_b)]^2} \times \Bigg\{kr\Bigg\{[J_{-(v+1)}(kr) + G_0J_{v+1}(kr)] \times \frac{\partial}{\partial v}[J_{-v}(kr) - G_0J_v(kr)] - [J_{-v}(kr) - G_0J_v(kr)]\frac{\partial}{\partial v}[J_{-(v+1)}(kr) + G_0J_{v+1}(kr)]\Bigg\} - [J_{-v}(kr) - G_0J_v(kr)]^2\Bigg\}_{r=r_b}^{r=r_a}, \quad (14)$$

and

$$P_m^{\mathrm{II}} = \frac{1}{2}\int_0^{r_a}[E_r^{\mathrm{III}}H_\phi^{*\mathrm{III}} - E_\phi^{\mathrm{III}}H_r^{*\mathrm{III}}]2\pi r\mathrm{d}r = \pi r_a[BV(kr_a)]^2\left(\frac{w}{p}\right)^2\left(\frac{\sin(\beta_m w/2)}{\beta_m w/2}\right)^2\left(\frac{\beta_m}{\omega\mu_0}\right) \times \Bigg\{\frac{1}{4}\Bigg[\left(\frac{k}{\gamma_m}\right)^2 + \left(\frac{m\beta_m}{\gamma_m^2 r_a} - \tan\Psi\right)^2 \times \left(\frac{F_m(\gamma_m r_a)}{F_m'(\gamma_m r_a)}\right)^2\Bigg] - \Bigg[\frac{F_{m+1}^2(\gamma_m r_a) + F_{m-1}^2(\gamma_m r_a)}{F_m^2(\gamma_m r_a)} - \frac{F_{m+2}(\gamma_m r_a) + F_{m-2}(\gamma_m r_a)}{F_m(\gamma_m r_a)}\Bigg] - m\frac{(\beta_m^2 + k^2)}{\gamma_m^2}\frac{[(m\beta_m/\gamma_m^2 r_a) \mp \tan\Psi]}{\gamma_m r_a \beta_m r_a}\frac{F_m(\gamma_m r_a)}{F_m'(\gamma_m r_a)}\Bigg\}. \quad (15)$$

3. Numerical results and discussion

The dispersion equation (9) is a very complicated transcendental equation including integrals associated with Bessel functions and the summations of an infinite series. Fortunately, the series converges rapidly as the term number m increases. For example, only four terms ($m = -2, -1, 0, 1$) are calculated, and the relative error of the solution may be less than 10^{-6}. In our calculation, we have taken seven terms into account ($|m| \leq 3$). Figure 2 shows the dispersion characteristics of the fundamental wave in the dielectric-loaded helical groove SWS for r_c/p=6.6, r_b/p=4.2, r_a/p=3.2, w/p=0.5 and ε_r=3.8.

As one would expect with a closed SWS, the helical groove structure exhibits a cut-off frequency, and can propagate fast waves and slow waves (Fig.2(a)). Moreover, it can be seen from Fig.2(b) that the curve of phase velocity versus frequency of the dielectric-loaded helical groove structure becomes flatter than that of the counterpart without dielectric-loading. This indicates that the beam-wave interaction will be maintained in a relatively wider frequency region in the former case. In other words, we can obtain a broader band amplifier in the dielectric-loaded helical groove SWS.

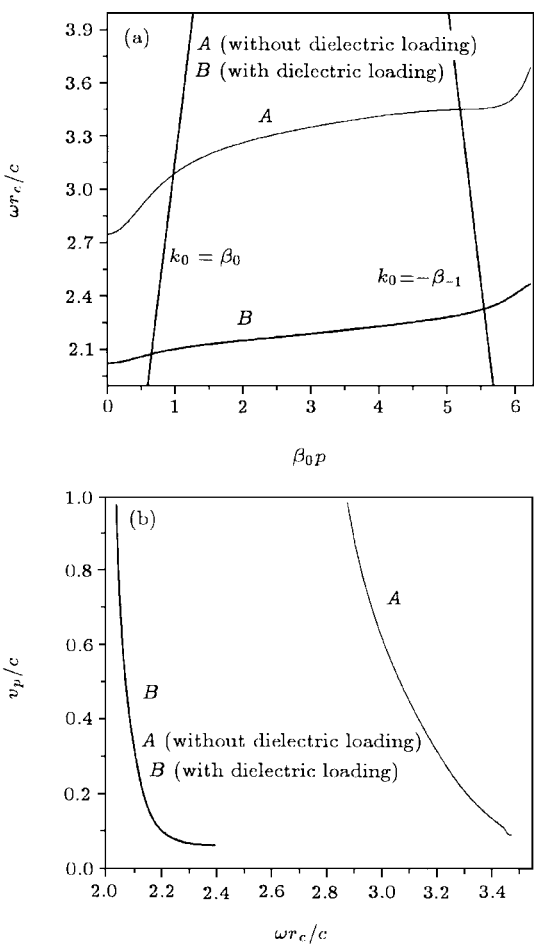


Fig.2. Dispersive characteristics of the dielectric-loaded helical groove SWS for r_c/p=6.6, r_b/p=4.2, r_a/p=3.2, w/p=0.5, ε_r=4.0: (a) $\omega r_c/c$-$\beta_0 p$ curves; (b) v_p/c-$\omega r_c/c$ curves.

The influence of the dielectric-loading on the coupling impedance is illustrated in Fig.3, in which the physical parameters are same as those in Fig.2. Here, the radius of the beam r_e is assumed to be $0.9r_a$. It is shown that the dielectric-loading reduces the coupling impedance of the fundamental wave. This decrease of coupling impedance is not desirable because it will cause a reduction of the gain and the efficiency of the tube. Therefore, the value of the relative permittivity of the dielectric should be properly chosen.

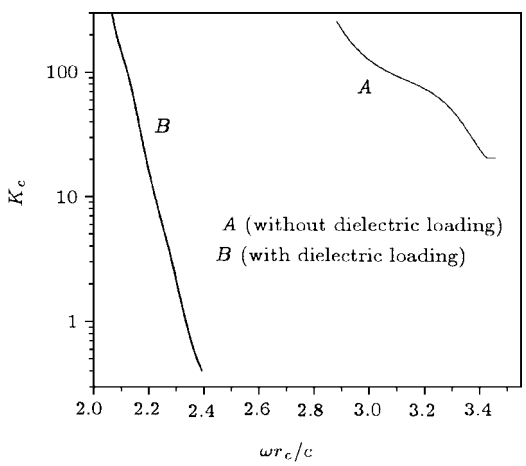


Fig.3. Coupling impedance of the dielectric-loaded structure (the structure parameters are the same as those in Fig.2).

In order to mitigate the effect of the dielectric-loading on coupling impedance, we examine the distribution of the longitudinal electric field E_z along the r direction, which reveals the nature of the beam-wave interaction. In Fig.4, the profiles of E_z are shown for several values of dielectric constant ε_r. The position marked by the dashed line is $r = r_a$. It is evident from Fig.4 that the field amplitude increases rapidly with the increase of r, and at $r = r_a$ it reaches an extremum for the case without dielectric-loading. Thus, in the general case without dielectric-loading, a thin hollow beam near r_a may be employed for high efficiency of the beam-wave interaction. We also observe that, when the structure is loaded with dielectric, the position of the maximal E_z is moved to the groove space (Fig.4). This is due to the fact that the loaded dielectric makes the electromagnetic energy concentrate inside the groove.[14] Then, the beam-hole position should be selected in the groove region to obtain high gain and high efficiency. In this case, multi-beams may be employed.

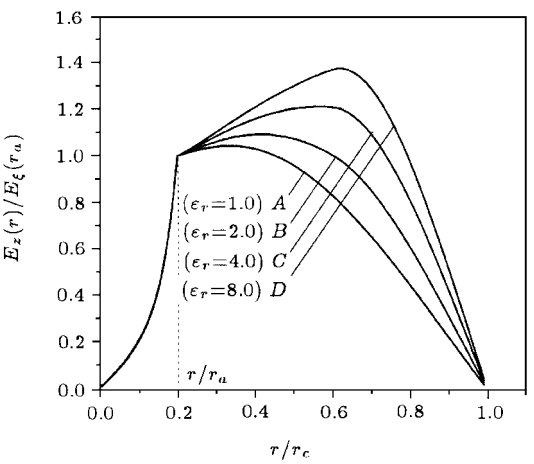


Fig.4. The longitudinal electric field profiles for several values of dielectric permittivity.

4. Conclusion

In this paper, we have presented a partial-dielectric-loaded helical groove waveguide as a slow-wave structure for a travelling wave tube and we put the emphasis on the effect of the dielectric parameters on the rf characteristics of the structure. It is shown that the dielectric-loading can make the structure less dispersive, but reduce the coupling impedance. In order to increase the gain and output power of the tube, the use of this type of structure with multi-beam holes lying at the groove wall is suggested.

References

[1] Epsztein B 1984 *IEDM'84* M486
[2] Wang W X, Yu G F and Wei Y Y 1997 *IEEE Trans. Microw. Theory Tech.* **45** 1689
[3] Waldron R A 1957 *J. Br. IRE.* **17** 577
[4] Nwachuku M A 1961 *PhD Dissertation* Department of Electrical Engineering, University of London
[5] Foulds K W H and Mansell J R 1964 *Proc. IEE* **111** 1789
[6] Liss C, Harper R and Puri M P 1988 *IEDM'88* M374
[7] Wei Y Y, Wang W X *et al* 2000 *Acta Phys. Sin.* **49** 949 (in Chinese)
[8] Wang W X, Lan Y H and Wei Y Y 2000 *Int. J. Infrared Millim. Waves* **21** 1617
[9] Wei Y Y, Wang W X and Sun J H 2000 *IEEE Microw. Guid. Wave Lett.* **10** 4
[10] Gai W 2000 *Conf. Digest of 25th Int. Conf. on Infrared and Millimeter Waves (Beijing, China)* M261
[11] Gai W, Conde M, Konecy R *et al* 1998 *Proc. 1997 Particle Accelerator Conference, IEEE* **1** M633
[12] Wang Z, Chen Q and Wu H 1999 *Acta Electron. Sin.* **27** 40 (in Chinese)
[13] Pierce J R 1950 *Traveling Wave Tubes* (Princeton, NJ: Van Nostrand)
[14] Qain B, Li C L and Liu Y G 1996 *Phys. Rev.* E **53** 1864